minerals

MDPI

Article

Preparation of Amino Functionalized Hydrophobic Zeolite and Its Adsorption Properties for Chromate and Naphthalene

Cheng Wang *, Shaozheng Leng, Yuan Xu, Qinyue Tian, Xuemeng Zhang, Liyun Cao and Jianfeng Huang *

School of Materials Science and Technology, Shaanxi University of Science and Technology, Xi'an 710021, China; stayme1111@163.com (S.L.); dylan5978@163.com (Y.X.); m18329381300@163.com (Q.T.); zhangxuemeng127@163.com (X.Z.); caoliyun@sust.edu.cn (L.C.)

* Correspondence: wangcheng@sust.edu.cn (C.W.); huangjf@sust.edu.cn (J.H.); Tel.: +86-29-8616-8688 (C.W.); Fax: +86-29-8616-8802 (C.W.)

Received: 24 February 2018; Accepted: 2 April 2018; Published: 5 April 2018

Abstract: Amino functionalized hydrophobic zeolite was prepared by modification of natural zeolite with 3-aminopropyltrimethoxysilane. X-ray diffraction, Fourier transform infrared analysis, thermal gravimetric analysis, Brunauer-Emmett-Teller surface areas, and element analysis were employed to investigate the structures of the samples. The water vapor adsorption method was used to determine the hydrophobicity of the samples. The adsorption properties of the samples for chromate and naphthalene were then investigated. The results showed that the silane modification had a negligible effect on the crystalline structure of zeolite while significantly decreasing the specific surface area and increasing the hydrophobicity of the zeolite sample. The functionalized zeolite samples exhibit higher adsorption capacity and removal rate on chromate and naphthalene as compared with the unmodified zeolite sample due to their specific amino functional group and hydrophobicity property.

Keywords: clinoptilolite; functionalization; hydrophobicity; chromate; naphthalene

1. Introduction

Natural zeolites are hydrated aluminosilicate porous minerals with valuable physicochemical properties, such as cation exchange, molecular sieving, catalysis, sorption etc. Application of natural zeolites for water and wastewater treatment is a promising environmental cleaning technique due to its advantages of low-cost, large quantities, good mechanical and thermal properties, and high sorption capacity for various contaminations [1,2]. In the past decades, utilization of natural zeolites has been focused on NH_4^+ [3], certain kinds of heavy metal ions [4], polar organic contaminations [5,6] etc. based on their properties of high cation exchange, polarity, and hydrophilicity.

Recent researches indicate that modifications of zeolites, such as ion exchange [7], surfactant/organosilane modification [8–10], and acid treatment [11,12] can significantly change the properties of zeolites, which greatly influence practical applications. Barquist and Larsen [13,14] successively functionalized silicate-1 and magnetic zeolite with 3-aminopropyltriethoxysilane ($NH_2(CH_2)_3Si(OC_2H_5)_3$, APTES) and found that the APTES functionalization increased negatively charged chromate adsorption due to its positively charged amino functional groups. However, only the amino group and its anionic ion removal property were noticed in this work while the hydrocarbonchain, its hydrophobicity and hydrophobic contamination removal property were overlooked. In addition, the high cost of the synthesized zeolite also partly limited its practical application.

In this paper, natural clinoptilolite was modified with 3-aminopropyltrimethoxysilane (APTMS) to form an amino functionalized hydrophobic zeolite adsorbent. The aim of this study was to enhance the

adsorptive properties of natural clinoptilolite towards anionic ions and hydrophobic contaminations. X-ray diffraction (XRD), Fourier transform infrared analysis (FTIR), thermal gravimetric analysis (TG), Brunauer-Emmett-Teller surface areas (BET method), and element analysis (organic carbon content) were employed to investigate the structures and components of the samples. The water vapor adsorption method was used to determine the wettability of the samples. Chromate and naphthalene were used to evaluate the adsorption property of the samples.

2. Experimental

2.1. Materials

The zeolite used in this study was purified natural clinoptilolite (<45 μm) obtained from Xinji, Hebei China. 3-aminopropyltrimethoxysilane (APTMS) (97%) was obtained from Hubei Wuda Organosilicon New Materials Co., Ltd. (Wuhan, China). Cyclohexane (99.5%) and naphthalene (98%) were obtained from Shanghai Aladdin Biochemical Technology Co., Ltd. (Shanghai, China). Potassium chromate (99.5%) was obtained from Xi'an Chemical Reagent Factory (Xi'an, China). An amount of 5.0 g of pre-dried (60 °C for 24 h) zeolite powders was added in 100 mL cyclohexane with different APTMS concentrations (5–80 wt % of zeolite powders). The system was placed in a stable temperature horizontal shaking bath and kept at 60 °C for 24 h with a speed of 120 r/min. The solid samples were filtered off the liquid dispersion and then successively washed with ethanol and distilled water several times, and finally dried at 60 °C for 24 h.

2.2. Sample Characterization

XRD patterns of the samples were recorded using a D/max-2200PCX diffractometer (Rigaku Corporation, Tokyo, Japan), with Cu Kα radiation and a graphite monochromator, operating at 44 mA and 40 kV. The step size was 0.02° 2θ, and the exposure time was 1 s per step. A VECTOR-22 FTIR spectrometer (Bruker Corporation, Karlsruhe, Germany) was used to obtain transmission Fourier transform infrared (FTIR) spectra of the samples in the wave number region of 4000–400 cm^{-1}, using the KBr pressed disk technique. Thermal gravimetric-differential thermogravimetry (TG-DTG) analysis was performed on STA409PC thermal analyzer (NETZSCH-Gerätebau GmbH, Selb, Germany) from room temperature to 600 °C at a heating rate of 10 K/min. The specific surface areas of the samples were determined using a Gemini VII2390 automated physisorption analyzer (Micromeritics Instrument Corp., Norcross, GA, USA) through N_2 adsorption/desorption. The total carbon content of the samples was determined using a VarioMICRO cube elemental analyzer (Elementar, Hanau, Germany).

2.3. Wettability Determination

The water vapor adsorption method was used to determine the wettability of the samples. An amount of 1 g of solids was placed in a temperature humidity chamber (BPS-50CL, Shanghai Yiheng Technical Co., Ltd., Shanghai, China). The weight change of the samples was measured under atmospheric conditions at 40 °C every 24 h until a constant weight was obtained, and the humidity was changed from 40% to 70% every 24 h.

2.4. Adsorption Experiments

The adsorption experiments were conducted using 50 mL polyethylene bottles in a Rotary mixer (MX-RL-E, SCILOGEX, Rocky Hill, CT, USA) with a rotational speed of 80 rpm. An amount of 5 g/L of natural clinoptilolite solids was added to chromate or naphthalene solutions. The initial chromate and naphthalene concentrations were 5–120 mg/L and 5–30 mg/L, respectively. The pH of the chromate solution was controlled at pH = 2 with 6 mol/L HCl solution for the purpose of protonation of the amine group in acidic solution [13]. The mixture was stirred for 1 h at room temperature (22.5 °C) and then centrifuged to separate the solid from the supernatant. The concentration of chromate and naphthalene in the obtained supernatant was analyzed using a UV-vis spectrophotometer (Unico

Instrument Co., Ltd., Shanghai, China). The detailed description of the procedure and calculation method can be found elsewhere [15].

The adsorption capacities were then obtained by mass balance calculations. The chromate and naphthalene uptakes, q_e (mg/g), were determined as:

$$q_e = (C_0 - C_e) \times V/W \quad (1)$$

and the removal rate was determined as:

$$R = (C_0 - C_e)/C_0 \times 100\% \quad (2)$$

where C_0 and C_e are the initial and final chromate/naphthalene concentrations (mg/L), respectively, V is the volume of solution (L) and W is the weight of adsorbent (g).

Two kinetic models including pseudo-first-order and pseudo-second-order equations were employed to investigate the characteristics of the adsorption kinetics. The pseudo-first-order model is given by

$$dq_t/dt = k_1(q_e - q_t) \quad (3)$$

where k_1 is the pseudo-first-order rate constant (min^{-1}) and q_e is the pseudo-equilibrium adsorption corresponding to the initial liquid concentration C_0. After integrating Equation (3) with the conditions $q_t = 0$, $t = 0$ and $q_t = q_t$, $t = t$, we have

$$\ln(q_e - q_t) = \ln q_e - k_1 t \quad (4)$$

The pseudo-second-order model is expressed as

$$dq_t/dt = k_2(q_e - q_t)^2 \quad (5)$$

where k_2 is the pseudo-second-order rate constant ($g \cdot mg^{-1} \cdot min^{-1}$). Similarly, the following equation can be obtained after integration:

$$t/q_t = 1/(k_2 q_e^2) + (1/q_e)t \quad (6)$$

Langmuir and Freundlich isotherm models have been widely applied to describe the adsorption isotherms. The Langmuir model assumes that adsorption occurs on a homogenous adsorbent surface of identical sites that are equally available and energetically equivalent with each site, carry equal numbers of molecules, with no interaction between adsorbate molecules. The equation is shown as:

$$q_e = q_{mon} K_L C_e/(1 + K_L C_e) \quad (7)$$

where q_{mon} is the maximum amount of adsorption corresponding to complete monolayer coverage on the surface (mg/g), K_L is the Langmuir constant related to the energy of adsorption (L/mg). The constants q_{mon} and K_L can be determined from the linearized form of the above equation:

$$1/q_e = 1/q_{mon} + 1/(K_L q_{mon} C_e) \quad (8)$$

For the Langmuir type adsorption process, the influence of the isotherm shape on whether adsorption is "favorable" or "unfavorable" can be classified by a separation factor or equilibrium parameter (R_L).

$$R_L = 1/(1 + K_L C_0) \quad (8)$$

where R_L is a dimensionless constant separation factor. The parameter R_L indicates the shape of the isotherm accordingly. The essential features of the Langmuir adsorption isotherm can be expressed in terms of a dimensionless constant called separation factor or equilibrium parameter (R_L). The R_L value

indicates the shape of the isotherm to be irreversible ($R_L = 0$), favorable ($0 < R_L < 1$), linear ($R_L = 0$) or unfavorable ($R_L > 1$).

The Freundlich isotherm assumes that the adsorption occurs on the heterogeneous surface at sites with different energy of adsorption and with non-identical adsorption sites that are not always available.

$$q_e = K_F C_e^{1/n} \quad (9)$$

where K_F is roughly an indicator of the adsorption capacity ($mg/g(mg/L)^n$), and a greater value of K_F means greater adsorption capacity. The term $1/n$ gives an indication of the favorability of adsorption and a value of $n > 1$ represents favorable adsorption condition.

The Freundlich model can be represented by the linear form as follows:

$$\ln q_e = \ln K_F + 1/n \times \ln C_e \quad (10)$$

A plot of $\ln q_e$ versus $\ln C_e$, gives a straight line with K_F and $1/n$ determined from the intercept and the slope, respectively.

3. Results

3.1. Characterization of the Samples

Figure 1 shows the total carbon contents of zeolite and functionalized zeolite samples and real quantities of APTMS loaded in the samples. The real quantities of APTMS loaded in the samples were calculated based on the carbon contents of the samples (20.08 wt % of carbon in amino silane). It is clear that the total carbon content and quantities of APTMS loaded in the zeolite samples gradually increase with the increase of the amino silane dosage. This suggests that the quantities of APTMS loaded in the zeolite samples directly depend on the additive dosage of the amino silane coupling agent.

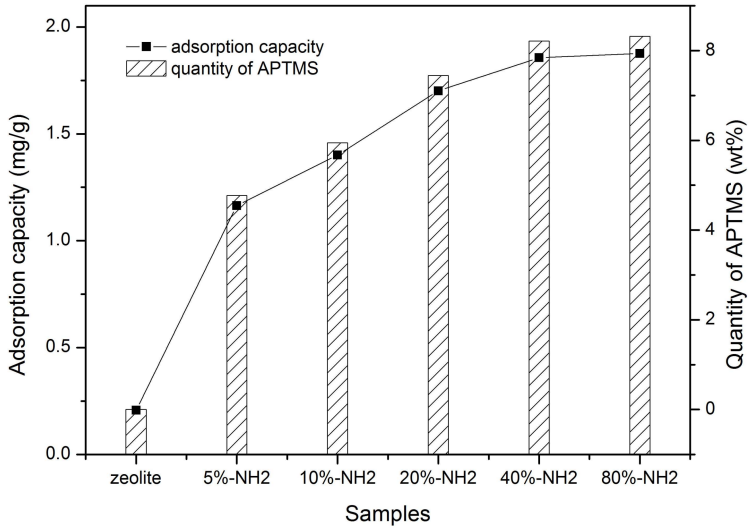

Figure 1. Total carbon contents of zeolite and amino functionalized zeolite samples and real quantities of 3-aminopropyltrimethoxysilane (APTMS) loaded in the samples.

Figure 2 shows the XRD patterns of zeolite and functionalized zeolite samples. XRD patterns indicate that natural zeolite consists of clinoptilolite with a small amount of montmorillonite. No change could be found in the XRD patterns of the functionalized zeolite samples compared with that of the unmodified zeolite sample.

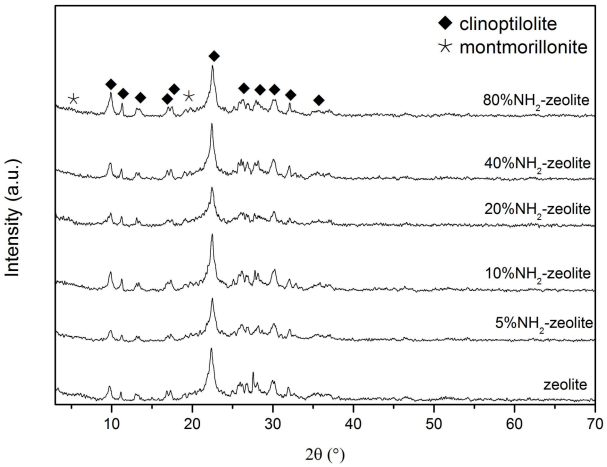

Figure 2. X-ray diffraction (XRD) patterns of zeolite and amino functionalized zeolite samples.

In order to further investigate the effect of silane modification on the structure of zeolite, the 20% amino functionalized zeolite sample was selected and characterized due to its relatively lower silane dosage and higher adsorption property.

Figure 3 shows the FTIR spectra of zeolite and 20% amino functionalized zeolite. For the FTIR spectrum of the zeolite sample, the peak at 3637 cm^{-1} corresponds to stretching vibration of Si–O(H)–Al [4]. A peak at 3426 cm^{-1} is due to vibration of the Si–OH bond. The 1646 cm^{-1} peak refers to deformation vibration of absorbed water. The peak at 1047 cm^{-1} corresponds to the stretching vibration modes of internal T–O bonds in TO_4 tetrahedra (T = Si and Al). The peaks at 793 and 468 cm^{-1} are assigned to the stretching vibration modes of O–T–O groups and the bending vibration modes of T–O bonds, respectively. In the spectrum of the amino functionalized zeolite sample, two peaks at 2934 and 2860 cm^{-1} correspond to the stretching vibration of the $–CH_2$ group and two peaks at 1567 and 1493 cm^{-1} refer to the formation vibration of the $–NH_2$ group [16]. In addition, it was found that the bond at 3426 cm^{-1} almost disappears in the amino functionalized zeolite sample.

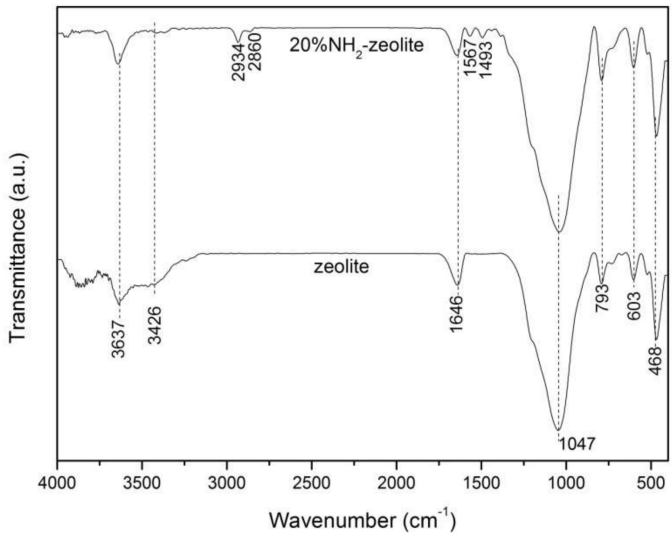

Figure 3. Fourier transform infrared analysis spectra of zeolite and 20% amino functionalized zeolite sample.

Figure 4 shows the TG-DTG curves (a) and N_2 adsorption-desorption isotherms (b) of zeolite and 20% amino functionalized zeolite. The TG curve of the zeolite sample indicates that the total

weight loss of the sample is 8.0%, which is attributed to removal of adsorption water, bound water, and structure water from the sample. Comparison of the TG-DTG curves of the amino functionalized zeolite and zeolite samples show that total weight loss of the functionalized sample is 2.4% higher than that of zeolite sample. In addition, a weight loss peak at 426.9 °C can be found in the DTG curve of the functionalized zeolite.

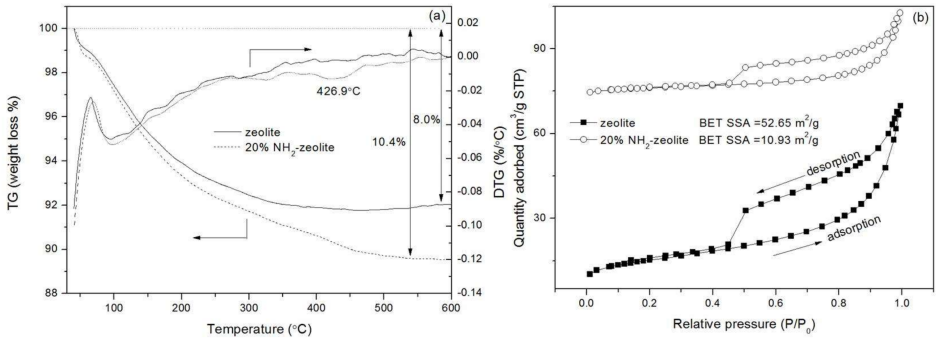

Figure 4. Thermal gravimetric and differential thermal gravimetric analysis (TG-DTG) curves (**a**) and N_2 adsorption-desorption isotherms (**b**) of zeolite and 20% amino functionalized zeolite sample; the isotherms for 20% amino functionalized zeolite are vertically offset by around 75 cm^3/g.

The shapes of adsorption-desorption isotherms and hysteresis loops of the zeolite and 20% amino functionalized zeolite correspond to the IV and H4 types, respectively (according to IUPAC). This proves the presence of slit-like mesopores in the zeolite samples [17,18]. In addition, the hysteresis loop of the zeolite sample significantly decreases after silane modification. The specific surface areas of samples were calculated from the adsorption isotherms using BET theory and the results indicate that the specific surface area of the unmodified zeolite sample is 57.65 m^2/g and the number is greatly reduced to 10.93 m^2/g for the functionalized zeolite.

3.2. Wettability of the Samples

Figure 5 shows the water vapor adsorption of zeolite and functionalized zeolite samples under humidity of 40–70%. It is clear that water vapor adsorption on the samples follows approximately linear dependence with humidity. Water vapor adsorption on the zeolite sample is obviously higher than that on the functionalized zeolite samples. As an example, water vapor adsorption on the zeolite sample under humidity of 70% is 84.18 mg/g while with the 20% amino functionalized zeolite sample it is only 23.82 mg/g. The decrease of water vapor adsorption suggests that silane modification significantly increases the hydrophobicity of zeolite.

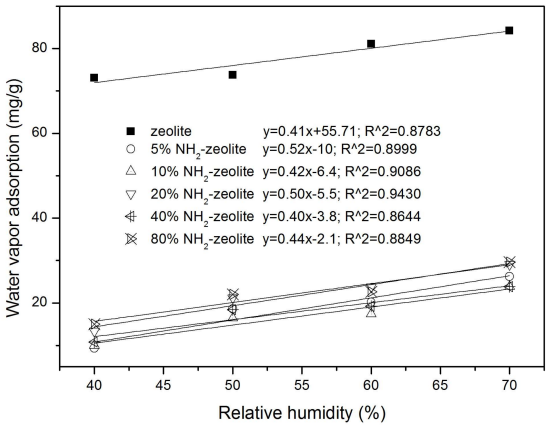

Figure 5. Water vapor adsorption of zeolite and amino functionalized zeolite samples under different humidities.

3.3. Adsorption Properties of the Samples

3.3.1. Adsorption of Chromate

The effect of the amino silane dosage on adsorption properties of the zeolite and amino functionalized zeolite samples towards chromate ions (40 mg/L) were investigated and the results are shown in Figure 6. It can be observed that the adsorption properties of the functionalized zeolite samples are significantly higher than that of the unmodified zeolite sample, and the adsorption properties gradually increase with the increase of amino silane dosage. The adsorption capacity and removal rate for the unmodified zeolite sample are 0.12 mg/g and 2.91%, while those for the 20% amino functionalized zeolite reach to 3.44 mg/g and 85.93%, respectively.

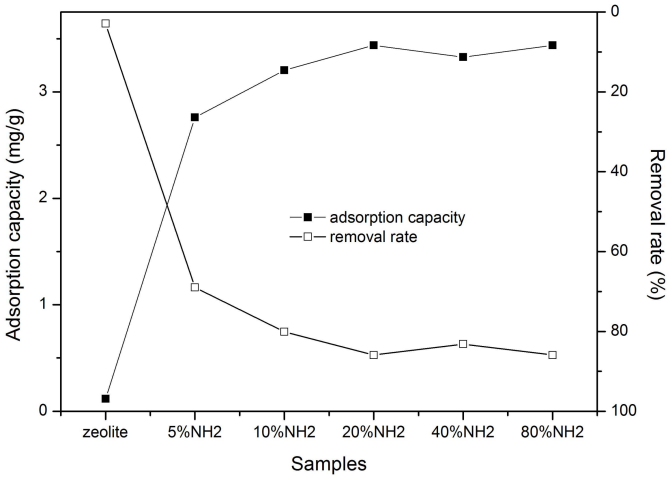

Figure 6. Adsorption properties of zeolite and amino functionalized zeolite samples with different silane dosage towards chromate ions.

The effect of adsorption time on adsorption properties of the zeolite and 20% amino functionalized zeolite towards chromate ions with initial concentration of 40 mg/L was investigated and the results are shown in Figure 7. It is clear that the functionalized zeolite sample takes only about 5 min to achieve equilibrium for adsorption of chromate ions. However, the zeolite sample has negligible adsorption property on chromate ions.

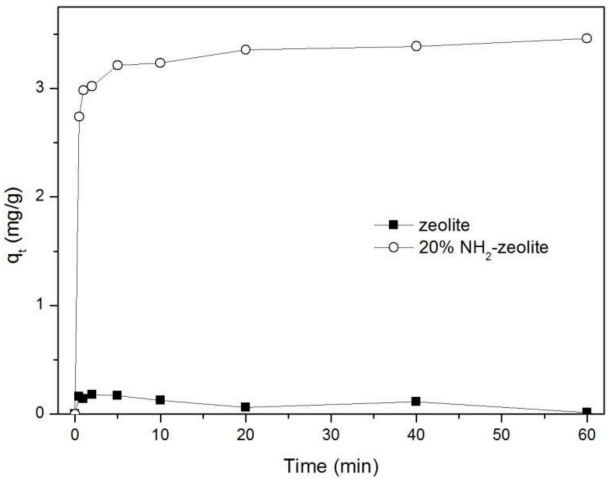

Figure 7. Adsorption properties of zeolite and 20% amino functionalized zeolite sample towards chromate ions at different adsorption times.

The pseudo-first-order (a) and pseudo-second-order (b) kinetic models for adsorption of chromate ions onto 20% amino functionalized zeolite are shown in Figure 8. It can be observed that the correlation coefficient (r^2) for the pseudo-first order is 0.8747. Moreover, the calculated q_e value (0.456 mg/g) does not agree with the experimental data (3.461 mg/g), showing that the adsorption of chromate on the functionalized zeolite is not a pseudo-first-order reaction [19]. The correlation coefficient (r^2) for the second-order kinetic model is 0.9998, which indicates that the adsorption system obeys the pseudo-second-order kinetic model. In addition, the calculated q_e value (3.459 mg/g) agrees very well with the experimental data. This suggests that adsorption of chromate ions on the amino functionalized zeolite samples is mainly chemisorption [19].

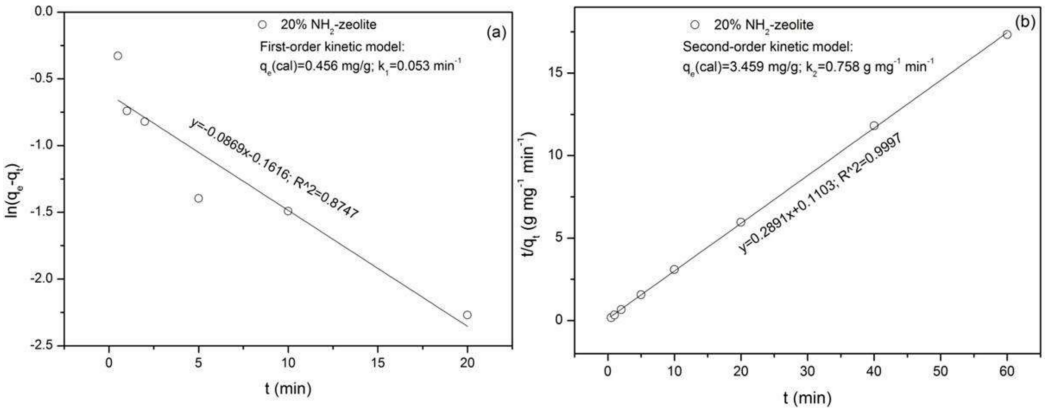

Figure 8. Plots of pseudo-first-order (**a**) and pseudo-second-order kinetic (**b**) models for adsorption of chromate ions onto 20% amino functionalized zeolite sample.

Figure 9 illustrates the isotherm for adsorption of chromate ions with different concentrations (5–120 mg/L) onto the 20% amino functionalized zeolite. The equilibrium adsorption results for the zeolite sample are not supplied due to its insignificant removal efficiency on chromate ions. The results show that the experimental maximum adsorption capacity of the functionalized zeolite towards chromate ions is about 9.49 mg/g.

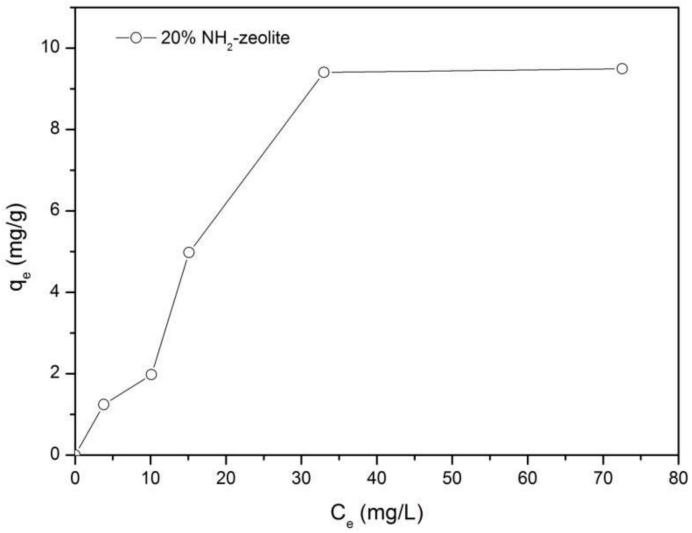

Figure 9. Isotherm for adsorption of chromate ions onto amino functionalized zeolite sample.

Figure 10 shows Langmuir and Freundlich plots for adsorption of chromate ions onto the 20% amino functionalized zeolite. Comparison of correlation coefficients (r^2) for the two models indicates

that the Langmuir model can fit the equilibrium isotherm well. It suggests that the adsorption of chromate ions onto the functionalized zeolite is a monolayer phenomenon [19]. The q_{mon} value for adsorption of chromate ions onto amino functionalized zeolite is 14.797 mg/g which is significantly higher than the experimental result. The separation factor R_L calculated from Equation (9) is 0.266 which indicates that the functionalized zeolite is favorable for adsorption of chromate ions. The Freundlich constant n is 1.296 which further suggests that chromate ions are favorably adsorbed by the functionalized zeolite.

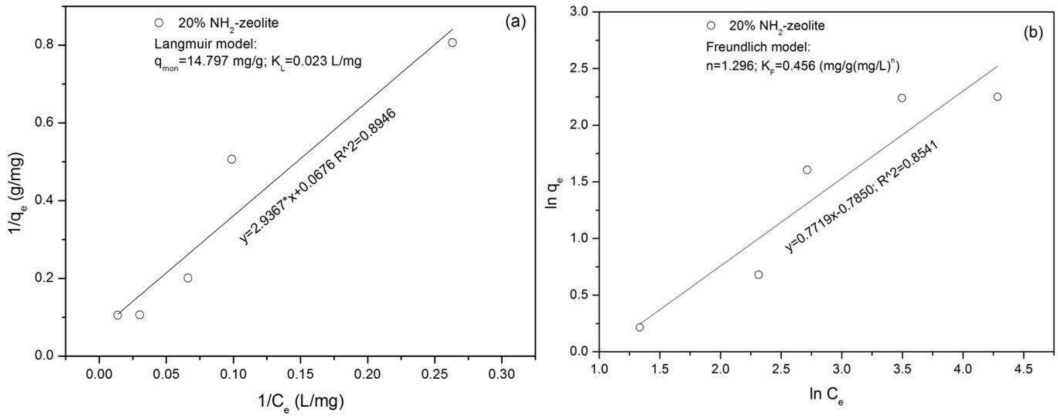

Figure 10. Langmuir (**a**) and Freundlich (**b**) plots for adsorption of chromate ions onto the amino functionalized zeolite sample.

3.3.2. Adsorption of Naphthalene

The effect of the amino silane dosage on adsorption properties of the zeolite and functionalized zeolite samples towards naphthalene (20 mg/L) was investigated and the results are shown in Figure 11. It is clear that the zeolite sample has a relatively good adsorption property on naphthalene with adsorption capacity of 1.63 mg/g and removal rate of 81.67%. The adsorption property of the functionalized zeolite samples towards naphthalene apparently improves. The adsorption capacity and removal rate for the 20% amino functionalized zeolite rise up to 1.88 mg/g and 93.95%, respectively.

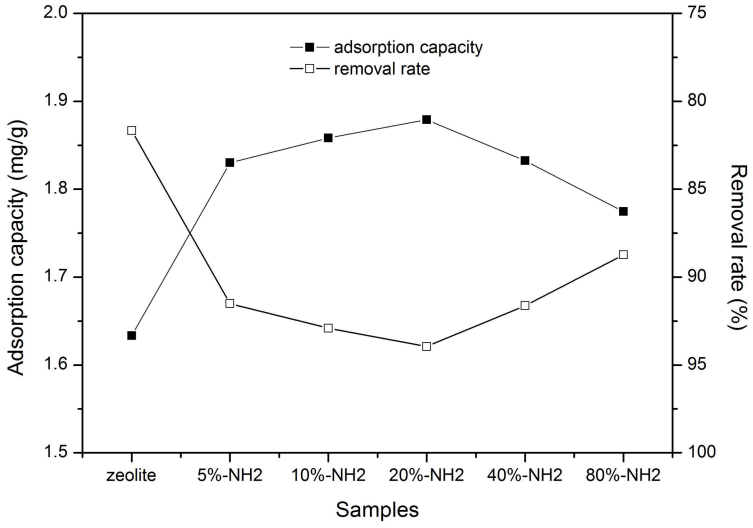

Figure 11. Adsorption properties of zeolite and amino functionalized zeolite samples with different silane dosage towards naphthalene.

The effect of adsorption time on adsorption properties of the zeolite and 20% amino functionalized zeolite towards naphthalene (20 mg/L) was investigated and the results are shown in Figure 12. It can be observed that both the zeolite and functionalized zeolite exhibit a high adsorption speed towards naphthalene while the adsorption speed of the functionalized zeolite is higher.

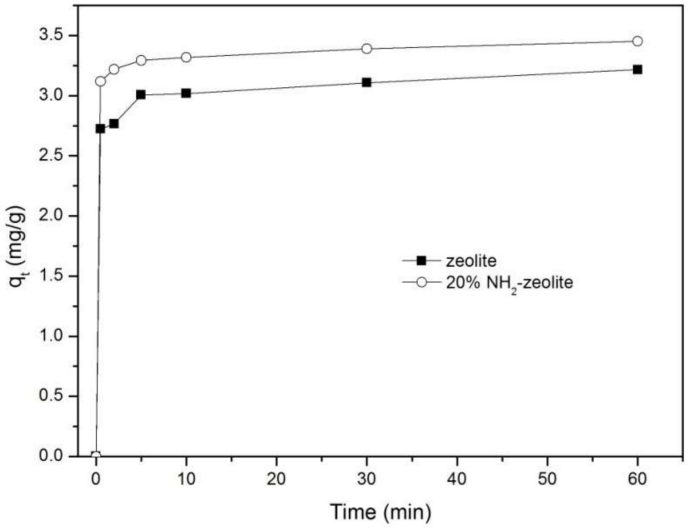

Figure 12. Adsorption properties of zeolite and 20% amino functionalized zeolite sample towards naphthalene at different adsorption times.

The pseudo-first-order (a) and pseudo-second-order (b) kinetic models for adsorption of naphthalene onto the zeolite and 20% amino functionalized zeolite are shown in Figure 13. It can be seen that the correlation coefficients (r^2) for the pseudo-first order are 0.7170 (zeolite) and 0.8629 (functionalized zeolite), respectively. This indicates that the adsorption of naphthalene on the zeolite and functionalized zeolite are not pseudo-first-order reaction. The second-order kinetic model exhibits higher correlation coefficients (r^2) for 0.9996 (zeolite) and 0.9999 (functionalized zeolite), respectively and this indicates that the adsorption system obeys the pseudo-second-order kinetic model. The calculated q_e value and k_2 for amino functionalized zeolite (3.457 mg/g and 1.142 g/mg/min) are higher than that for zeolite (3.221 mg/g and 0.706 g/mg/min). This suggests that amino silane modification increases the adsorption capacity and adsorption speed for naphthalene.

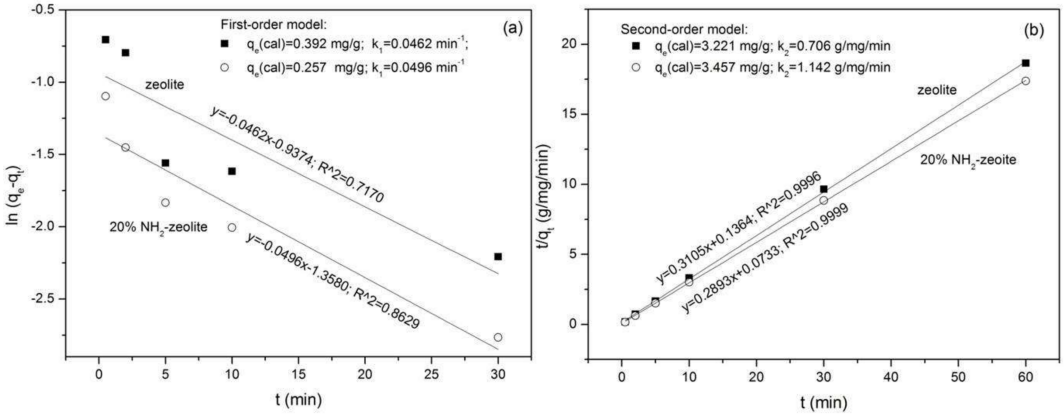

Figure 13. Plots of pseudo-first-order (**a**) and pseudo-second-order kinetic models (**b**) for adsorption of naphthalene onto zeolite and the 20% amino functionalized zeolite sample.

Figure 14 illustrates the isotherm for adsorption of naphthalene with different concentrations (5–30 mg/L) onto the zeolite and 20% amino functionalized zeolite. It is clear that the adsorption ability of the amino functionalized zeolite sample on naphthalene is higher than that of the zeolite sample. However, it was found that the adsorptions of naphthalene onto the two zeolite samples had not reached equilibrium state. Theoretically, this problem can be solved by increasing the initial concentration of naphthalene or decreasing the dosage of sorbent. Unfortunately, it is hard to prepare a naphthalene solution with high concentration due to the low water solubility of naphthalene. Further work to prepare a relatively higher concentration should be done, e.g., adding some amount of butanol to increase the solubility of naphthalene [20].

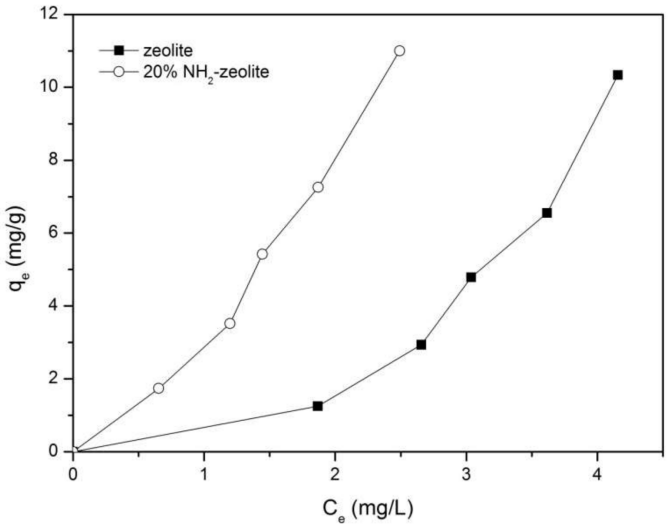

Figure 14. Isotherm for adsorption of naphthalene onto the zeolite and amino functionalized zeolite samples.

Figure 15 shows Langmuir and Freundlich plots for adsorption of naphthalene onto the zeolite and amino functionalized zeolite. Although the Langmuir model for the equilibrium isotherm exhibits high correlation coefficients (0.9659 for zeolite and 0.9923 for functionalized zeolite), the calculated Langmuir constants of q_{mon} and k_1 are negative values. This indicates the inadequacy of the isotherm model to explain the adsorption process [21]. The Freundlich model is applicable and can fit the isotherm well. It was found that the Freundlich constants n and K_F for functionalized zeolite (0.717 and 3.043) are both higher than that for the zeolite sample (0.382 and 0.241). This illustrates that the amino silane modification increases the adsorption property of zeolite on naphthalene.

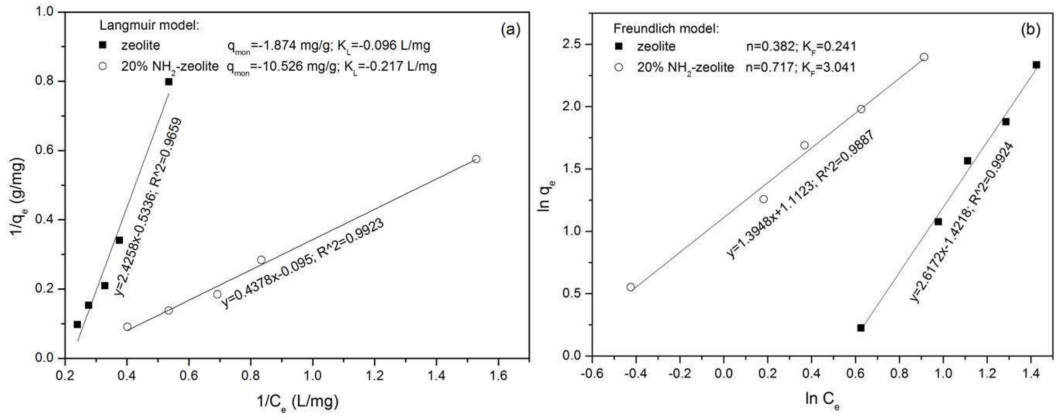

Figure 15. Langmuir (**a**) and Freundlich (**b**) plots for adsorption of naphthalene onto the zeolite and amino functionalized zeolite samples.

4. Discussion

From the total carbon content results, it was found that the real quantities of APTMS in the zeolite samples were obviously lower than the additive dosage of APTMS, e.g., only 7.45 wt % of APTMS was loaded in the 20% amino functionalized zeolite sample with the additive dosage of APTMS of 20 wt %. This is probably due to the limited silanol groups (active site for silane-zeolite reaction) in the zeolite sample. The XRD results suggest that the silane modification has negligible effect on the crystalline structure of zeolite, which is similar to previous reports [22]. The FTIR results confirm the occurrence of amino silane coupling agent in the functionalized zeolite sample based on the new peaks corresponding to $–CH_2$ and $–NH_2$ groups. Moreover, the disappearance of the peak at 3426 cm^{-1} for the functionalized zeolite sample demonstrates amino functionalization through Si–OH bonds. The TG-DTG results are consistent with the FTIR results which further prove the presence of silane coupling agent in the sample. The N_2 adsorption-desorption results show that the hysteresis loop of the zeolite sample significantly decreases after silane modification and the specific surface area of the functionalized zeolite sample is greatly reduced. This is probably due to the location of the silane coupling agent in the mesopores of zeolite [23]. Similar results were reported by Muir et al. [18].

Water vapor adsorption results show that the zeolite sample adsorbs a significantly high amount of water vapor, which may be due to its aluminosilicate framework and surface silanol groups with high polarity and hydrophilicity. Water vapor adsorptions on the amino functionalized zeolite samples were greatly reduced compared with that on the zeolite sample, and this is attributed to the hydrophobic hydrocarbon chain (propyl group) belonging to the silane coupling agent.

The characterization and water vapor adsorption results confirm that the 3-aminopropyltrimethoxysilane with $–OCH_3$ groups can react with the –OH groups on zeolite and thus form an amino functionalized zeolite. The amino group can ionize in acidic conditions and thereby become positive charged. In addition, the hydrocarbon chain of the silane coupling agent makes the surface of zeolite hydrophobic. This amino functionalized hydrophobic zeolite can be used to remove anionic ions (e.g., chromate ions) and hydrophobic contaminations (e.g., naphthalene) which was proved by the adsorption experiments. A schematic for modification of natural zeolite and the adsorption process of the amino functionalized hydrophobic zeolite on chromate and naphthalene is shown in Figure 16.

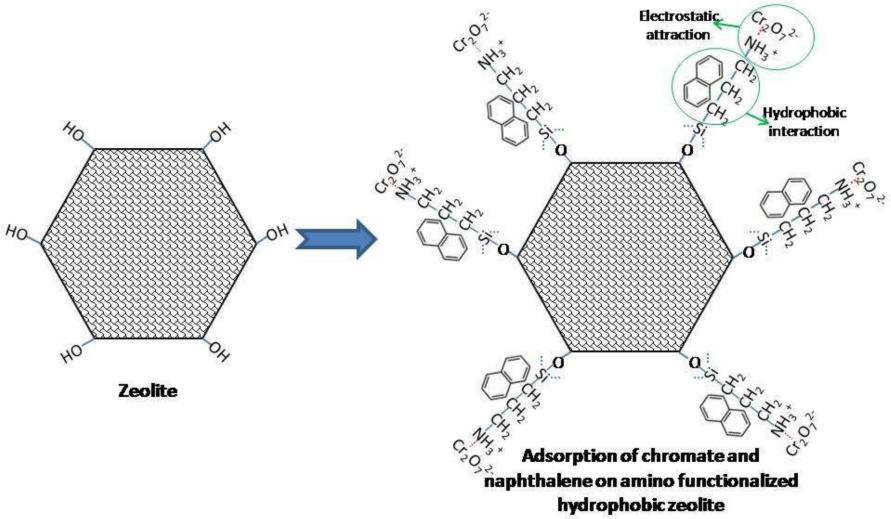

Figure 16. Schematic for modification of natural zeolite and the adsorption process of the amino functionalized hydrophobic zeolite on chromate and naphthalene.

5. Conclusions

Amino functionalized hydrophobic zeolite was successfully prepared by modifying natural zeolite with 3-aminopropyltrimethoxysilane. The amino functionalized zeolite samples exhibited higher adsorption capacity and removal rate for the chromate ions and naphthalene compared with the unmodified zeolite sample. The adsorption of chromate ions obeyed the pseudo-second-order kinetic model and the equilibrium isotherm fitted the Langmuir model well. The adsorption of naphthalene obeyed the pseudo-second-order kinetic model and the equilibrium isotherm had a good fit for the Freundlich model. This amino functionalized hydrophobic zeolite sorbent appears to be a good candidate for removal of anionic ions and hydrophobic contamination. However, further work to improve the adsorption capacity of the functionalized zeolite towards anionic ions and hydrophobic contamination should still be carried out.

Acknowledgments: The project was supported by the National Natural Science Foundation of China (No. 51604170), Chinese Postdoctoral Science Foundation (No. 2016M602936XB), Natural Science Foundation of Shaanxi Provincial Department of Education (No. 16JK1092), Shaanxi Natural Science Foundation of China (No. 2013JQ6007), and Foundation of Shaanxi University of Science and Technology (No. BJ12-18).

Author Contributions: Cheng Wang conceived and designed the experiments, analyzed the data, wrote and revised the paper; Shaozheng Leng performed the experiments and analyzed the data; Yuan Xu, Qinyue Tian and Xuemeng Zhang performed the experiments; Liyun Cao and Jianfeng Huang analyzed the data and revised the paper.

Conflicts of Interest: The authors declare no conflict of interest.

References

1. Wang, S.; Peng, Y. Natural zeolites as effective adsorbents in water and wastewater treatment. *Chem. Eng. J.* **2010**, *156*, 11–24. [CrossRef]
2. Misaelides, P. Application of natural zeolites in environmental remediation: A short review. *Microporous Mesoporous Mater.* **2011**, *144*, 15–18. [CrossRef]
3. Franus, W.; Wdowin, M. Removal of ammonium ions by selected natural and synthetic zeolites. *Gospod. Surowcami Miner.* **2010**, *26*, 133–148.
4. Korkuna, O.; Leboda, R.; Skubiszewska-Zie, J.; Vrublevs'ka, T.; Gun'ko, V.M.; Ryczkowski, J. Structural and physicochemical properties of natural zeolites: Clinoptilolite and mordenite. *Microporous Mesoporous Mater.* **2006**, *87*, 243–254. [CrossRef]
5. Yousef, R.I.; El-Eswed, B.; Al-Muhtaseb, A.H. Adsorption characteristics of natural zeolites as solid adsorbents for phenol removal from aqueous solutions: Kinetics, mechanism, and thermodynamics studies. *Chem. Eng. J.* **2011**, *171*, 1143–1149. [CrossRef]
6. Liang, H.J.; Gao, H.; Kong, Q.Q.; Chen, Z.X. Adsorption equilibrium and kinetics of tetrahydrofuran + water solution. *J. Chem. Eng. Data* **2006**, *51*, 119–122. [CrossRef]
7. Gómez-Hortigüela, L.; Pinar, A.B.; Pérez-Pariente, J.; Sani, T.; Chebude, Y.; Díaz, I. Ion-exchange in natural zeolite stilbite and significance in defluoridation ability. *Microporous Mesoporous Mater.* **2014**, *193*, 93–102. [CrossRef]
8. Jin, X.; Yu, B.; Chen, Z.; Arocena, J.M.; Thring, R.W. Adsorption of Orange II dye in aqueous solution onto surfactant-coated zeolite: Characterization, kinetic and thermodynamic studies. *J. Colloid Interface Sci.* **2014**, *435*, 15–20. [CrossRef] [PubMed]
9. Wang, C.; Li, Y.; Shi, H.S.; Huang, J.F. Preparation and characterization of natural zeolite supported nano TiO_2 photocatalysts by a modified electrostatic self-assembly method. *Surf. Interface Anal.* **2015**, *47*, 142–147. [CrossRef]
10. Bonaccorsi, L.; Bruzzaniti, P.; Calabrese, L.; Proverbio, E. Organosilanes functionalization of alumino-silica zeolites for water adsorption applications. *Microporous Mesoporous Mater.* **2016**, *234*, 113–119. [CrossRef]
11. Wang, X.; Plackowski, C.A.; Nguyen, A.V. X-ray photoelectron spectroscopic investigation into the surface effects of sulphuric acid treated natural zeolite. *Powder Technol.* **2016**, *295*, 27–34. [CrossRef]
12. Wang, C.; Cao, L.Y.; Huang, J.F. Influences of acid and heat treatments on the structure and water vapor adsorption property of natural zeolite. *Surf. Interface Anal.* **2017**, *49*, 1249–1255. [CrossRef]

13. Barquist, K.; Sarah, C.L. Chromate adsorption on amine-functionalized nanocrystalline silicalite-1. *Microporous Mesoporous Mater.* **2008**, *116*, 365–369. [CrossRef]
14. Barquist, K.; Sarah, C.L. Chromate adsorption on bifunctional, magnetic zeolite composites. *Microporous Mesoporous Mater.* **2010**, *130*, 197–202. [CrossRef]
15. Wang, C.; Shi, H.S.; Li, Y. Synthesis and characteristics of natural zeolite supported Fe^{3+}-TiO_2 photocatalysts. *Appl. Surf. Sci.* **2011**, *257*, 6873–6877. [CrossRef]
16. Majoul, N.; Aouida, S.; Bessaïs, B. Progress of porous silicon APTES-functionalization by FTIR investigations. *Appl. Surf. Sci.* **2015**, *331*, 388–391. [CrossRef]
17. Sing, K.S. Reporting physisorption data for gas/solid systems with special reference to the determination of surface area and porosity (Recommendations 1984). *Pure Appl. Chem.* **1985**, *57*, 603–619. [CrossRef]
18. Muir, B.; Bajda, T. Organically modified zeolites in petroleum compounds spill cleanup-Production, efficiency, utilization. *Fuel Process. Technol.* **2016**, *149*, 153–162. [CrossRef]
19. Bandura, L.; Kolodyńska, D.; Franus, W. Adsorption of BTX from aqueous solutions by Na-P1 zeolite obtained from fly ash. *Process Saf. Environ. Prot.* **2017**, *109*, 214–223. [CrossRef]
20. Şener, S.; Özyılmaz, A. Adsorption of naphthalene onto sonicated talc from aqueous solutions. *Ultrason. Sonochem.* **2010**, *17*, 932–938. [CrossRef] [PubMed]
21. Öztürk, N.; Bektaş, T.E. Nitrate removal from aqueous solution by adsorption onto various materials. *J. Hazard. Mater.* **2004**, *112*, 155–162. [CrossRef] [PubMed]
22. Sayilkan, H.; Erdemoğlu, S.; Sener, S.; Sayilkan, F.; Akarsu, M.; Erdemoğlu, M. Surface modification of pyrophyllite with amino silane coupling agent for the removal of 4-nitrophenol from aqueous solutions. *J. Colloid Interface Sci.* **2004**, *275*, 530–538. [CrossRef] [PubMed]
23. Bouvy, C.; Marine, W.; Sporken, R.; Su, B.L. Nanosized ZnO confined inside a Faujasite X zeolite matrix: Characterization and optical properties. *Colloid Surf. A* **2007**, *300*, 145–149. [CrossRef]